Facile, productive and cost-effective synthesis of a novel tetrazine-based iron oxide nanoparticle for targeted image contrast agents and nanomedicines

Marco M. Meloni • Stephen Barton • Alexandru Chivu • Juan C. Kaski • Wenhui Song • Taigang He

Abstract We have developed an operationally simple, time and cost-effective protocol to produce a novel tetrazine-based iron oxide nanoparticle using commercially available and inexpensive materials. Our protocol proceeds at room temperature and uses Hexafluorophosphate Azabenzotriazole Tetramethyl Uronium, a well-known, widely used reagent for the large-scale industrial production of important pharmaceuticals. The nanoparticles obtained have a diameter range between 16 and 21 nm and showed no toxicity against endothelial cell lines. The tetrazine moiety on the nanoparticle surface could potentially allow further attachment of specific targeting vectors by using so-called copper-free click chemistry. We therefore anticipate that our protocol can represent a significant breakthrough in the future development and commercialization of improved, tissue-specific contrast agents and drug delivery for clinical diagnosis, monitoring and therapy of diseases at an asymptomatic stage.

Keywords Diagnosis • Magnetic Resonance Imaging • Iron Oxide Nanoparticles • Copper-free click Chemistry • Bioconjugation • Synthesis

Introduction

Since their discovery (Ohgushi, 1978), Iron Oxide Nanoparticles (IONPs) have emerged as powerful tools for a wide scope of applications such as in the fields of biolabeling, medical diagnostics, and therapy (Colombo et al. 2012). In particular as contrast agents for magnetic resonance imaging (MRI), IONPs have attracted enormous attention. IONPs have a transverse relaxivity which increases at higher magnetic fields, resulting in enhanced signal-to-noise ratio with lower dosages (Mishra et al. 2016). The use of IONPs for diagnostic imaging is therefore expected to increase steadily. Unlike Gd-based contrast agents (CAs), IONPs have proven safe with some systems already approved for clinical use (Schmitz et al. 2001; Trivedi et al. 2004). With the recent advent of molecular imaging (Meloni et al. 2017), IONPs are increasingly used for the preparation of targeted CAs, allowing non-invasive visualization of biomolecules which are the signatures of diseases in specific body tissues, both *in vivo* and in real time. The preparation of these targeted CAs firstly involves coating of the IONPs surface with a biocompatible, clinically approved polymer, followed by its functionalization with a targeting vector which allows tissue specificity (A. M. Morawski et al. 2005).

This process, so-called standard bioconjugation, uses well-established synthetic chemistry and involves the formation of stable chemical bonds. Despite being reliable, this method can lead to low yields and produce toxic byproducts, resulting in expensive, time-consuming purifications and toxicological screenings. A number of years may therefore be required for the translation, large scale production and commercialization of targeted, nanoparticle-based CAs into the clinical market.

Copper-free click reactions recently emerged as a powerful, time-saving bioconjugation strategy to prepare targeted CAs (Devaraj and Weissleder 2011; McKay and Finn 2014). Copper-free click reactions are operationally simpler and proceed at room temperature. They eliminate the use of cytotoxic copper catalysts (Baskin JM et al. 2007) and are inert to both water and oxygen. They also generate minimal, inoffensive byproducts, providing the best yield with the highest reaction rates. Copper-free click reactions can proceed in living organisms, allowing the targeting of biomolecules with high specificity without altering any native biochemical process. Among the arsenal of available copper-free click reactions, the Inverse Electron Demand Diels Alder (IEDDA) reaction stands out as the most promising one for its rapid reaction rate and generation of safe, inert nitrogen as the only byproduct (Oliveira et al. 2017). IEDDA reactions also involve tetrazines and cycloalkenes, both of which are easier substrates to prepare if compared to azadibenzocyclooctynes (DIBACs) (Debets et al. 2010) and biarylazacyclooctynones (BARACs) (Kuzmin et al. 2010). Despite such significant advantages, the preparation of targeted, nanoparticle-based CAs using IEDDA is a relatively unexplored field. A possible reason is a shortage of reliable protocols to prepare tetrazine-based IONPs. Therefore, the

Marco M. Meloni • Juan C. Kaski • Taigang He
The Cardiology Academy Group, St George's University of London, Cranmer Terrace, SW17 0RE, London, UK.

Marco M. Meloni • Stephen Barton
School of Pharmacy and Chemistry, Kingston University, Penhryn Road, KT1 2EE, London, UK.

Alexandru Chivu • Wenhui Song
UCL Centre for Biomaterials, Division of surgery & Interventional Science, University College London, Pond Street, NW3 2PS, London, UK.

Taigang He
Royal Brompton Hospital, Imperial College London, London, UK.

Marco M. Meloni (✉) • Taigang He (✉)
The Cardiology Academy Group, St George's University of London, Cranmer Terrace, SW17 0RE, London, UK.

e-mail: mmeloni@sgul.ac.uk
e-mail: the@sgul.ac.uk

identification of novel, green and efficient ways to prepare these functional nanoparticles can accelerate the development of improved contrast agents for diagnosis and therapy. In this paper we designed and synthesized a novel route to a tetrazine-bound nanoparticle **4** (Scheme 1).

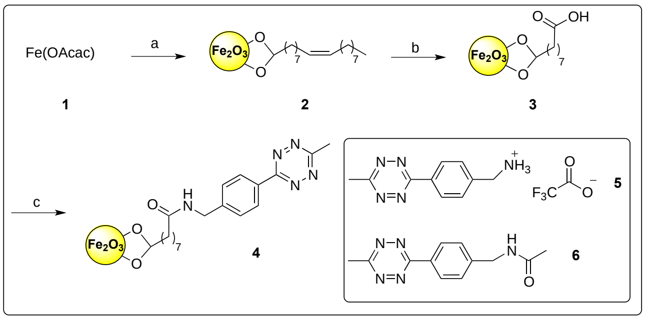

Scheme 1 (a) Oleic acid, oleylamine, phenyl ether (b) BTAC, $KMnO_4$ (c). Tetrazine **5**, HATU, DIPEA, CH_2Cl_2, at room temperature.

As illustrated above, our strategy involved the loading of a tetrazine moiety to nanoparticles **3** using Hexafluorophosphate Azabenzotriazole Tetramethyl Uronium (HATU), a readily available, inexpensive and well-known reagent. Our overall approach to nanoparticles **4** can be exploited for the future production of improved contrast reagents, with potential application also in the fields of nanomedicine.

Results and discussion

In this work, we successfully designed and developed an operationally simple, economical and productive approach to produce a novel tetrazine-decorated IONP **4** (Scheme 1, page 2). Our protocol is reproducible by taking an advantage of well-established chemistry and usages of building blocks **3** and **5**, both accessible via established published protocols (Herranz et al. 2008; Evans et al. 2014). Nanoparticles **4** were obtained via coupling between carboxylic acid IONPs **3** and tetrazine-based amine **5** (Scheme 1, page 2). Our method builds upon the reaction between a carboxylic acid and an amine, which produces extremely stable chemical bonds even in a biological environment and is one of the most robust, known reactions in synthetic chemistry (Jaradat, 2018). During this process a challenge also emerged due to the presence of the paramagnetic core both in **3** and **4**, which excluded quantitative reaction monitoring via NMR. Therefore, we first decided to validate the chemistry using acetic acid as a surrogate for nanoparticles **3**. We wanted a fast, high yielding protocol to obtain model compound **6**. After unsuccessful attempts to prepare this latter using N-hydroxysuccinimide (NHS) and 1-Ethyl-3-(3-dimethylaminopropyl)carbodiimide (EDC) in water (Herranz et al. 2008), we found that the system HATU/DIPEA/CH_2Cl_2 afforded **6** in 92% yield after only 3 hours.
We therefore adopted this method for the synthesis of nanoparticles **4**. Coupling between **3** and **5** was performed with HATU and DIPEA in CH_2Cl_2, affording the desired nanoparticles **4**. We found this method both safe and operationally simple for many reasons. Firstly, HATU is an established chemical which is widely used during large scale synthesis of pharmaceuticals. Several reports of HATU applications have showcased its use in the synthesis of promising drug candidates (Dunetz et al. 2016 and references cited herein). Secondly, a simple filtration/washing cycle can be used to purify and isolate nanoparticles **4**. Thirdly, the reaction also proceeded both at room temperature and in presence of relatively safe chemicals. Finally, our approach is highly reproducible. As a proof, we repeated the synthesis three times, obtaining nanoparticles **4** with the same zeta potentials in all cases (see Table 1). Yields of nanoparticles **4** were 91%, 88% and 90% for repetitions 1-3 respectively. We therefore believe that our approach to nanoparticles **4** can be feasible for a scale-up production. The tetrazine grafted on IONP render a nano-platform for conjugating a diverse range of biomolecules or drugs via copper-free click chemistry. This strategy has advantages of simplifying chemical synthesis, avoiding cytotoxic copper catalysts and generating a system to detect biomarkers in live cells with improved sensitivity. One such example is the nanoparticle-antibody conjugate developed to image extracellular receptors in cancer cells (Haun et al. 2010).

Table 1. Zeta potentials found for nanoparticles precursor **3**, tetrazine bound IONPs **4** and yields obtained.

Sample (repeat)	IONPs **3** (mV)	IONPs **4** (mV)
1	-37.6	-20.5
2	-41.1	-16.1
3	-42.9	-18.1

With nanoparticles **4** successfully prepared, we then decided to assess their shape and average size. These parameters are relevant in assessing IONPs sensitivity for biosensing applications. As a proof, in 2013 Kolhatkar et al. demonstrated that cubic and spherical nanoparticles display different sensitivities due to their different contact areas. With this in mind, we obtained TEM images of IONPs **4** (Figures 1a-d). It can be seen that the particles are spherical in shape with a size range between 16 and 21 nm.

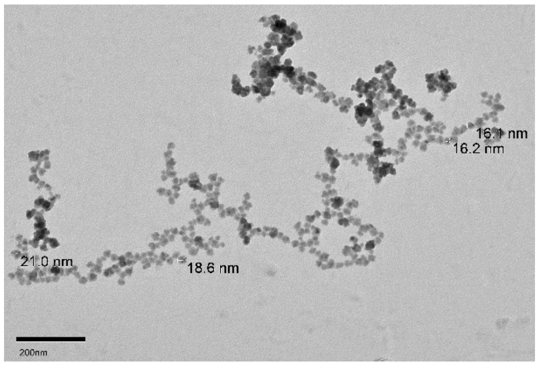

(1a)

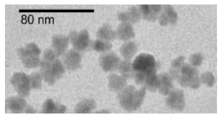

(1c)

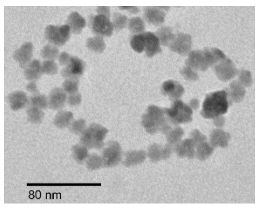

(1b)

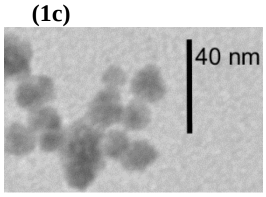

(1d)

Figures 1a-d. TEM Images of nanoparticles **2**

Once that both shape and size of the nanoparticles were assessed, we moved to establish their magnetic properties.

We were particularly interested in the saturation magnetization value because this is another key indicator in assessing IONPs sensitivity for biosensing applications (Colombo et al. 2012).

Magnetization curves were performed on a solid sample. IONPs **4** showed a paramagnetic behaviour with a saturation magnetization value of 1.49E-03 emu/g (Figure 2), confirming also that IONPs **4** present a degree of surface functionalisation.

Fig 2. Magnetization curve of IONPs **4** at 310K

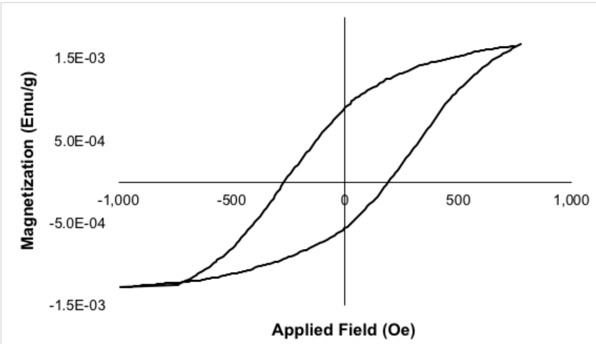

To further demonstrate the potential applicability of nanoparticles **4** in pre-clinical and clinical fields, we felt mandatory to perform toxicological screenings. After being cultured in the presence of nanoparticles **4** at various concentrations for one to three days, both metabolic activity (Figure 3) and total DNA of HUVECs (Figure 4) were performed, with no cytotoxicity or changes in cell viability and morphology encountered.

Fig. 3 Metabolic profiles of HUVEC cells treated at different concentrations of IONPs **4**.

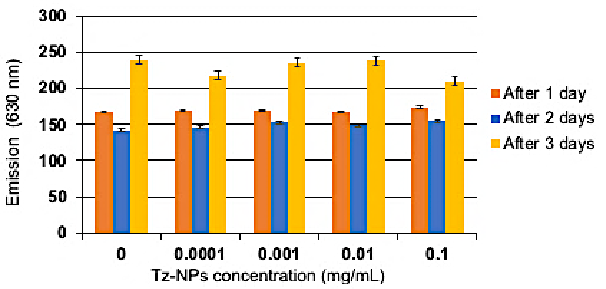

Fig. 4 Total DNA of HUVEC cells treated at different concentrations of IONPs **4**.

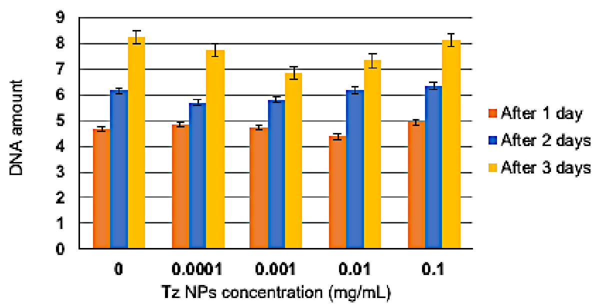

These results strongly suggest that targeted contrast reagents based on IONPs **4** can be safely used in pre-clinical and clinical imaging or magnetic-nanomedicine.

The relaxation rate is another key parameter in the applicability of nanoparticles **4** in preclinical and clinical fields. We plan to obtain this parameter as a part of our future applications *in vivo*, and the results will be reported in due course.

Conclusions

We have developed an operationally simple, high-yielding and cost-effective protocol to produce a novel class of low toxicity, tetrazine-based IONPs. Our protocol is reproducible and the tetrazine motif can be exploited for the preparation of conjugated biomolecules or drug molecules for targeted-based contrast agents or nanomedicine by using all the strengths of the well-known copper-free click chemistry. Targeted magnetic nanoparticle-based contrast agents and nanomedicines are rapidly emerging into the preclinical and clinical fields. We therefore anticipate that our method can represent an invaluable breakthrough and provides a multi-functional nanoparticle platform for the large-scale production and commercialization of improved, tissue specific contrast agents or magnetic nanomedicine for the clinical diagnosis and therapy of diseases at an asymptomatic stage.

Conflicts of interest

None to declare

Acknowledgements

This work is supported by the British Heart Foundation [FS/15/17/31411 to M. M. M.].

References

Baskin JM, Prescher JA, Laughlin ST, Agard NJ, Chang PV, Miller IA, Lo A, Codelli JA, Bertozzi CR (2007). Copper-free click chemistry for dynamic in vivo imaging. Proc Natl Acad Sci USA 104: 16793-16797. doi: 10.1073/pnas.0707090104

Colombo M, Carregal-Romero S, Casula MF, Gutierrez L, Morales MP, Bohm IB, Heverhagen JT, Prosperi D, Parak WJ (2012) Biological applications of magnetic nanoparticles Chem Soc Rev 41:4306-4334 https://doi:10.1039/c2cs15337h

Debets MF, van Berkel SS, Schoffelen S, Rutjes FP, van Hest JC, van Delft FL (2010) Aza-dibenzocyclooctynes for fast and efficient enzyme PEGylation via copper-free (3+2) cycloaddition ChemComm 46:97-99 https://doi:10.1039/b917797c

Devaraj NK, Weissleder R (2011) Biomedical Applications of Tetrazine Cycloadditions Acc Chem Res 44:816-827 https://doi:10.1021/ar200037t

Dunetz JR, Magano J, Weisenburger GA (2016) Large-Scale Applications of Amide Coupling Reagents for the Synthesis of Pharmaceuticals Org Process Res Dev 20:140-177 https://doi:10.1021/op500305s

Evans HL, Nguyen QD, Carroll LS, Kaliszczak M, Twyman FJ, Spivey AC, Aboagye EO (2014) A bioorthogonal (68) Ga-labelling strategy for rapid in vivo imaging ChemComm 50:9557-9560 https://doi:10.1039/c4cc03903c

Haun JB, Devaraj NK, Hilderbrand SA, Lee H, Weissleder R (2010) Bioorthogonal chemistry amplifies nanoparticle binding and enhances the sensitivity of cell detection Nature Nanotechnonogy 5:660-665 https://doi:10.1038/nnano.2010.148

Herranz F, Morales MP, Roca AG, Vilar R, Ruiz-Cabello J (2008) A new method for the aqueous functionalization of superparamagnetic Fe_2O_3 nanoparticles Contrast Media Mol Imaging 3:215-222 https://doi:10.1002/cmmi.254

Jaradat DMM (2018) Thirteen decades of peptide synthesis: key developments in solid phase peptide synthesis and amide bond formation utilized in peptide ligation Amino Acids 50:39-68 https://doi:10.1007/s00726-017-2516-0

Kolhatkar AG, Nekrashevich I, Litvinov D, Willson RC, Lee TR (2013). Cubic Silica-Coated and Amine-Functionalized FeCo Nanoparticles with High Saturation Magnetization. Chem Mater, 25:1092-1097 https://doi: 10.1021/cm304111z

Kuzmin A, Poloukhtine A, Wolfert MA, Popik VV (2010) Surface Functionalization Using Catalyst-Free Azide−Alkyne Cycloaddition Bioconjugate Chem. 21:2076-2085 https://doi:10.1021/bc100306u

McKay CS, Finn MG (2014) Click chemistry in complex mixtures: bioorthogonal bioconjugation Chem Biol 21:1075-1101 https://doi:10.1016/j.chembiol.2014.09.002

Meloni MM, Barton S, Xu L, Kaski JC, Song W, He T (2017) Contrast agents for cardiovascular magnetic resonance imaging: an overview J Mater Chem B 5:5714-5725 https://doi:10.1039/c7tb01241a

Mishra SK, Kumar BS, Khushu S, Tripathi RP, Gangenahalli G (2016) Increased transverse relaxivity in ultrasmall superparamagnetic iron oxide nanoparticles used as MRI contrast agent for biomedical imaging Contrast Media Mol Imaging 5:350-361. https://doi: 10.1002/cmmi.1698

Morawski AM, Lanza GA, Wickline SA (2005) Targeted contrast agents for magnetic resonance imaging and ultrasound Curr Opin Biotechnol 16:89-92 https://doi:10.1016/j.copbio.2004.11.001

Ohgushi M, Nagayama K, Wada A (1978) Dextran-magnetite: A new relaxation reagent and its application to T2 measurements in gel systems J Magn Reson (1969) 29:599-601 https://doi.org/10.1016/0022-2364(78)90018-5

Oliveira BL, Guo Z, Bernardes GJL (2017) Inverse electron demand Diels-Alder reactions in chemical biology Chem Soc Rev 46:4895-4950 https://doi:10.1039/c7cs00184c

Schmitz SA, Taupitz M, Wagner S, Wolf K-J, Beyersdorff D, Hamm B (2001) Magnetic resonance imaging of atherosclerotic plaques using superparamagnetic iron oxide particles J Magn Reson Im 14:355-361 https://doi:10.1002/jmri.1194

Trivedi RA, U-King-Im JM, Graves MJ, Kirkpatrick PJ, Gillard JH (2004) Noninvasive imaging of carotid plaque inflammation Neurology 63:187-188 https://doi:10.1212/01.wnl.0000132962.12841.1d

Facile, productive and cost-effective synthesis of a novel tetrazine-based iron oxide nanoparticle for targeted image contrast agents and nanomedicines

Marco M. Meloni • Stephen Barton • Alexandru Chivu • Juan C. Kaski • Wenhui Song • Taigang He

Experimental

This section has two parts. The first one illustrates the chemical synthesis and characterization of our nanoparticles **4.** The second part contains the toxicity assays and the protocols used for growing cell cultures. Each section contains also the specific materials and equipment used for the analysis. The synthesis required also nanoparticles **3** and tetrazine **5**, which have been obtained following published protocols (Herranz et al. 2008; Evans et al. 2014). The synthetic route to **3** and **5** is illustrated in Schemes 2 and 3.

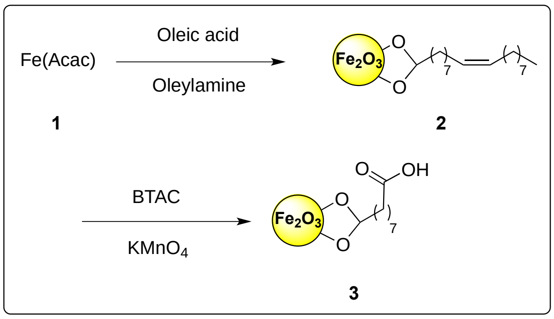

Scheme 2. Synthetic route to nanoparticles **3**

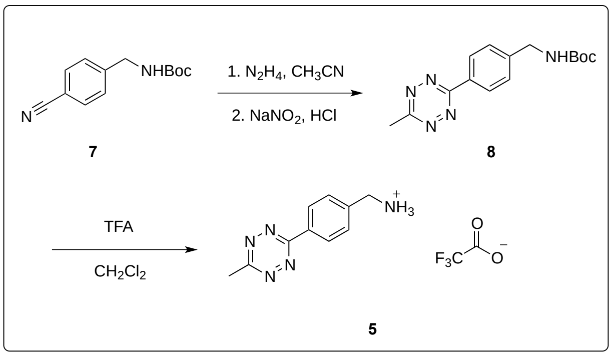

Scheme 3. Synthetic route to tetrazine **5**

Solvents and chemicals were purchased from commercial sources (Sigma Aldrich, Alfa Aesar, Acros) and used without further purification. Flash chromatography was performed on silica gel (Merck 60 F254, 230-400 mesh). Thin Layer Chromatography (TLC) was performed on Merck glass-backed plates coated with silica (0.2 mm, 60 F254). The presence of the compounds on the plates was detected by their exposure to ultraviolet light (λ = 254 nm) or immersion into a basic solution containing 10% $KMnO_4$. Nuclear Magnetic Resonance (NMR) spectra were recorded on a Bruker AV-400 instrument at 400 (or 100) MHz. Chemical shifts (δ) are quoted in parts per million (ppm). Transmission Electron Microscopy (TEM) images were performed using a Hitachi H7100 Microscope (0.3 nm point resolution, Tungsten hairpin filament). Magnetic measurements were performed using a Quantum Design MPMS-7 magnetometer. Zeta potentials were obtained with a Malvern Nano S90 instrument.

Preparation and characterization of N-(4-(6-methyl-1,2,4,5-tetrazin-3-yl)benzyl)acetamide **(6)**

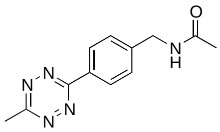

A microwave vial was charged with a stirring bar, (4-(6-methyl-1,2,4,5-tetrazin-3-yl)phenyl)methanaminium 2,2,2-trifluoroacetate **5** (20.0 mg, 0.06 mmol), CH_2Cl_2 (0.5 mL) and HATU (24.0 mgs, 0.06 mmol). The vial was then sealed and acetic acid (4.0 mg, 0.06 mmol) was added, followed by di-isopropylethylamine (DIPEA, 60 µL, 0.19 mmol). The resulting purple solution was then stirred at room temperature for 3 hours before being added of AcOEt (20 mL). The organics were then washed with brine, 1M HCl (10 mL), saturated Na_2CO_3 (15 mL) brine (15 mL) and dried (Na_2SO_4). Removal of the solvent and chromatography on silica (CH_2Cl_2 CH_3OH 95:5) afforded **6** as a bright purple solid (14.1 mg, 92%). Spectroscopic data were consistent with the structure.

Marco M. Meloni • Juan C. Kaski • Taigang He
The Cardiology Academy Group, St George's University of London, Cranmer Terrace, SW17 0RE, London, UK.

Marco M. Meloni • Stephen Barton
School of Pharmacy and Chemistry, Kingston University, Penhryn Road, KT1 2EE, London, UK.

Alexandru Chivu • Wenhui Song
UCL Centre for Biomaterials, Division of surgery & Interventional Science, University College London, Pond Street, NW3 2PS, London, UK.

Taigang He
Royal Brompton Hospital, Imperial College London, London, UK.

Marco M. Meloni (✉) • Taigang He (✉)
The Cardiology Academy Group, St George's University of London, Cranmer Terrace, SW17 0RE, London, UK.

e-mail: mmeloni@sgul.ac.uk
e-mail: the@sgul.ac.uk

^{1}H NMR (400 MHz, CDCl$_3$) δ: 8.56 (d, *J* = 8.5 Hz, 2H), 7.50 (d, *J* = 8.5 Hz, 2H), 5.86 (s, 1H), 4.56 (d, *J* = 6.0 Hz, 2H), 3.10 (s, 3H), 2.09 (s, 3H).

Preparation and characterization of tetrazine nanoparticles **(4)**

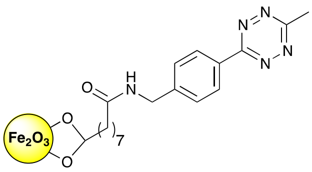

A microwave vial was charged with nanoparticles **3** (3.0 g), (4-(6-methyl-1,2,4,5-tetrazin-3-yl)phenyl)methanaminium 2,2,2-trifluoroacetate **5** (4.8 g, 15.3 mmol), HATU (5.7 g, 15.3 mmol) and CH_2Cl_2 (50 mL). DIPEA (8.1 mL, 45.0 mmol) was then added, the system sealed and the vial shaken at room temperature for 24 hours. The suspension was then centrifuged and the purple supernatants removed. The nanoparticles were then further washed with fresh CH_2Cl_2 (50 mL each time) until the supernatants were colourless and showed absence of starting materials (by TLC analysis, CH_2Cl_2 CH_3OH 90:10). The solid was then collected and dried under high vacuum at 60 °C to afford nanoparticles **4** as a light pink amorphous solid. Nanoparticles **4** were analysed by TEM and their zeta potential obtained (Table and Figure 1, page 2, main article).

Cytotoxicity test protocols

Unless otherwise stated, all the following protocols were performed using sterilized equipment. Endothelial cell medium, umbilical vein endothelial cells (HUVECs), Phosphate Buffered Saline (PBS) and Trypsin were purchased from commercial sources (PromoCell GmbH, Germany) and used without further purification. Metabolic assay was performed using AlamarBlue™ (Resazurin, AB, Serotec Ltd, Kidlington, UK). Total DNA assay was performed via the bis-benzimide (Hoechst 33258) quantitation method (see Sigma Aldrich Technical bulletin and references cited herein). Cells metabolic activity was established via UV readings by using a Fluoroskan Ascent FL multiwall plate reader (ThermoLab Systems).

Cells expansion culture

The following two-step protocol was used:
Step A. A vial containing frozen HUVECs (-78 °C) was gradually warmed to room temperature. Contents were pipetted out and transferred into a 50 mL falcon tube containing fresh endothelial cell growth medium (20 mL). After vortexing (1 minute) and centrifuging (1200 rpm, 5 min), the supernatants were removed and the pellet reconstituted in endothelial cell growth medium (20 mL). The vortexing-centrifugation cycle was repeated another two times (3 times overall). Fresh endothelial medium (20 mL) was added to the pellet and the resulting suspension transferred into a sterilized T-150 flask. The system was then put into an incubator (37° C, 1% CO_2); at regular intervals (48 hours) the old medium was removed, cells washed with warm PBS (37 °C, 3×20 mL, 3 min) and fresh endothelial medium (20 mL) was added.
Step b. Once the required confluency was reached (>90%, 4-5 days typically required), the cell medium was removed and cells washed with warm PBS (37° C, 3×20 mL, 3 min). After PBS removal, a solution of Trypsin-EDTA was added (5 mL) and the system put into the incubator. Upon complete cell detachment (3-5 minutes required, floating observed via light microscope), the cell suspension was transferred into a falcon tube and 20 mL of fresh medium was added. After centrifugation (1200 rpm, 5 minutes) the supernatants were removed and fresh medium (30 mL) was added to the cell pellet. The system was vortexed for 1 minute and the suspension partitioned into three T-150 flasks (10 mL each), which were put into the incubator (37° C 1% CO_2). Step B was then repeated until the required amounts of cells were obtained (16 passages).

Metabolic assay (Alamar Blue)™

Each well (of a 25 wells array) was loaded with the following:

1. A HUVECs suspension (100 μL, optimised initial density 5.45×10^5 cells/mL).
2. The appropriate volume of endothelial cell medium.
3. The required amount of nanoparticles solution (from a 3mg/mL stock solution in water).

Each of the 5 columns had the following nanoparticles concentration: 0 (control), 0.1, 1, 10 and 100 μg /mL and the total volume in each well was 1 mL.
After the required incubation period (1, 2 or 3 days at 37 °C, 1% CO_2) the supernatants were discarded and the cells washed with warm PBS (3 × 1mL, 3 minutes). A solution of AlamarBlue™ (400 μL, 10% in HUVEC medium) was then added to each well and the plates returned to the incubator (37° C 1% CO_2). After 2 hours the supernatants were removed and transferred to a 96-well microtiter plate (Note: a hypodermic needle was used to eliminate any eventual bubbles from the solution surfaces). The solutions were then analysed spectrophotometrically and the presence of the resorufin (the metabolic product of Alamar Blue™, λ_{ex} 580 nm, λ_{em} 630 nm) was quantified in each case.